

## DYNAMIC BEHAVIOR OF AN ACTIVE DAMPER

**Rafael Luís Teixeira\***  
rafael@mecanica.ufu.br

**Francisco Paulo Lépore Neto\***  
flepore@mecanica.ufu.br

**José Francisco Ribeiro\***  
jrribeiro@mecanica.ufu.br

\*Federal University of Uberlândia – College of Mechanical Engineering - Campus Santa Mônica 38400-089, Uberlândia-MG.

**Abstract.** This paper presents a validation methodology of the dynamic behavior of an active damper. The damper has two flexible metallic bellows connected to a rigid reservoir filled with fluid. When one of the bellows is connected to a vibrating structure a periodic flow passes through a variable internal orifice and the damping effect is produced. The size of the orifice is adjusted by a control system that positions the conical core into a conical cavity. The device finite element computational model was developed considering the fluid - structure iteration, and the lagrangean-eulerian formulation. The bellows are represented like two pistons with elastic suspensions, the valve body and its conical cores are assumed rigid. To validate the proposed model experimental tests and numerical simulations are accomplished in the time domain, applying harmonic excitations. The results are compared by curves that relate the damping factor with the size of the orifice. This paper also presents a reduced second order dynamic model for the damper which is suitable for applications where real time control is required. This simple model parameters are identified by an analysis on the frequency domain, using impulsive excitation force for the constant orifice (passive system) as for the variable orifice (active system). A fuzzy controller was designed to simulate the operation of the active system.

**Keywords.** Active damper, finite element, fluid/structure interaction, fuzzy controller.

### 1. Introduction

In several industrial applications it is necessary to absorb structural vibration energy, mainly when impulsive forces without any repetition pattern excites the mechanical system. In these cases, the passive absorbers has low efficiency, because they are only projected for a specific operating condition. Frequently, hydraulic piston actuators are used where large damping forces are required. However, the implementation, operation and maintenance of this type of solution are very expensive. These active suspensions are used by high performance vehicles and represent a significant amount of the car price. The current passive shock absorbers used on regular vehicles are designed for a nominal behavior and don't allow damping factor adjustments in function of the pavement type or even for comfort or stability operating conditions. New conceptions of vibration absorbers were proposed, investigated and tested in the last years. Some designs of active shock absorbers and dampers are presented here. Kipling (1999), Hagopian et al. (1999), Giliomee and Els (1998) developed shock absorbers systems based on hydraulic piston whose variable orifice is controlled by an electrodynamic valve. Oh and Onoda (2002) used metallic flexible bellows and electro and magneto-rheologic fluids.

The proposed active damper consists of two parts: a piezoelectric actuator system controls the valve opening; and a hydraulic-mechanical system generates the damping force. The hydraulic circuit contains a volumetric accumulator, a variable orifice, and a metallic cylindrical bellows. The bellows is flexible in the axial direction and its extremities are connected at two points of the vibrating structure. The vibrating motion, applied in the bellows axial direction, pumps the internal fluid through the valve orifice. The displaced fluid volume travels between the bellows and the accumulator. The flow restriction caused by the valve yield pressure gradients in hydraulic circuit depending of the orifice size. This internal pressure applied on the bellows transversal area generates the damping force that acts on the structure. The signal of the fluid velocity at the orifice changes opposed to de relative velocity applied to the bellows by the vibrating structure. The system becomes active because the valve closure can be adjusted by a position control system that uses a linear displacement piezoelectric actuator. The main objective of the work is to incorporate variable damping to the mechanical system, associated to each specific position of the valve; that is, a new shock absorber can be set at each sampling time of the state variables. This rate depends on the time response of the actuator, on the external excitations and on the desired dynamic performance of the vibratory system.

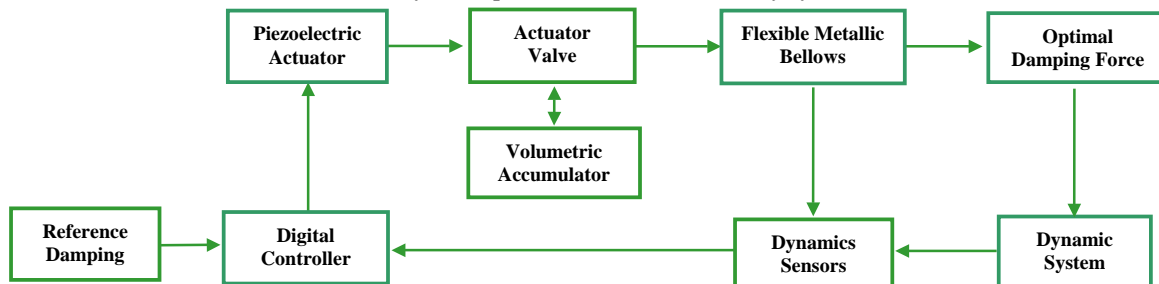


Figure 1: Block Diagram of the proposed active damper components

In the diagram shown in Fig.1, it is assumed that the flexible metallic bellow is attached to a dynamic vibratory system and that all state variables are measurable by appropriate sensors. Then, considering one reference damping coefficient and the associated system state, a digital controller will command the piezoelectric actuator that will position the flow regulator valve. Due to a control action, the resulted orifice size will set the fluid velocity, producing the damping force. The bellows expansion and contraction movements produce pressure variations inside the hydraulic circuit. The product of the internal pressure in the bellows by its cross section area results in a value of the damping force that depends on the control action applied to the valve. To avoid structural collapse of the bellows, the closure of the valve must be limited so that the internal pressure is always inferior to the maximum allowable pressure. The volumetric accumulator can be a pressure vase endowed with an internal pneumatic lung. Adjusting the pressure in the lung can set the nominal static pressure in the hydraulic circuit. The solution adopted was the use of a second bellows as the volumetric accumulator. The efficiency of this device is strongly dependent on the fluid viscosity and on the absence of mixed bubbles of gas dissolved in the oil. To solve this problem a parallel circuit with a vacuum pump can provide a preliminary remove the gas bubbles that are present in the working fluid. The choice of suitable value of the static nominal pressure in the hydraulic circuit can prevent the dissolved gas bubble generation in the low-pressure region of the circuit.

Some initial parameters were specified for the design and construction of the active damper prototype. A commercial metallic bellows was specified. It supports internal pressures up to 3.3 MPa, has an effective cross section area of 383 mm<sup>2</sup>, can generate axial loads up to 1300 N with a margin of safety of 25 %. The stroke of the bellows is in range of -8 mm up to 6 mm. The valve was designed to apply damping forces varying from - 800 N to 800 N. The piezoelectric actuator has a displacements range equal to 0.5 mm, and supports forces up to 570 N, as a function of the applied voltage in the frequency band from zero to 480 Hz. This paper is organized as follows: the finite element model of the hydraulic circuit that considers the interaction fluid-structure is presented; the active damper device prototype is shown and some experimental tests in the time domain are used to validate the experimental and simulation models; the active damper is characterized in the frequency domain and using optimizations tools, and a reduced order dynamic model is estimate using the experimental FRFs; finally, numeric simulations are done with a passive (fixed orifice) and active (variable orifice). For the active system a fuzzy controller was designed.

## 2. Finite element model of the hydraulic circuit

The hydraulic circuit model is developed by the finite element technique. As shown in Fig.2, the vibrations applied at the left end of the bellows imposes a known velocity to the fluid that is in contact with its internal end surface. At the right end of the hydraulic circuit a constant pressure, equal to the nominal static pressure is imposed. The volumetric accumulator is not shown in this figure. The valve orifice has conic shape. The orifice size can be adjusted by moving the conical core in the axial direction. In this region the fluid will reach higher velocities. When the bellows contracts the pressure will increase at the region located at the left side of the core and will be reduced at its right side. If the bellows expands, the pressure distribution will be reversed. To impose displacement in the fluid it used a piston in the amount and other in opposite side of valve to simulate the second bellows, characterizing the interaction fluid-structure. This model is used to determine the velocity and pressure fields developed in the fluid. By integrating the pressure on the core surface (excluding the actuator rod) the net force acting on the valve core is determined. Applying the same procedure on the left end surface of the bellows, the effective damping force acting on the vibrating structure can be calculated. The computational model of the hydraulic circuit was developed using the module FLOTTRAN CFD, Computational Fluid Dynamics, of the computational program ANSYS, considering the K -  $\epsilon$  model of turbulence, developed by Launder and Spalding (1974). According to the geometric characteristics of the problem, an axi-symmetric finite element model can be assembled. Figure 2 shows the configuration of the system components and the mesh geometry constructed with the FLUID141-2D quadrilateral finite elements. The mesh is refined at the central region around the valve core, where higher velocity gradients are expected to occur, like showed on Figure 03. The mesh was composed by 2741 elements, since this configuration provides the numerical convergence for the velocity and pressure fields, with reasonable number of iterations

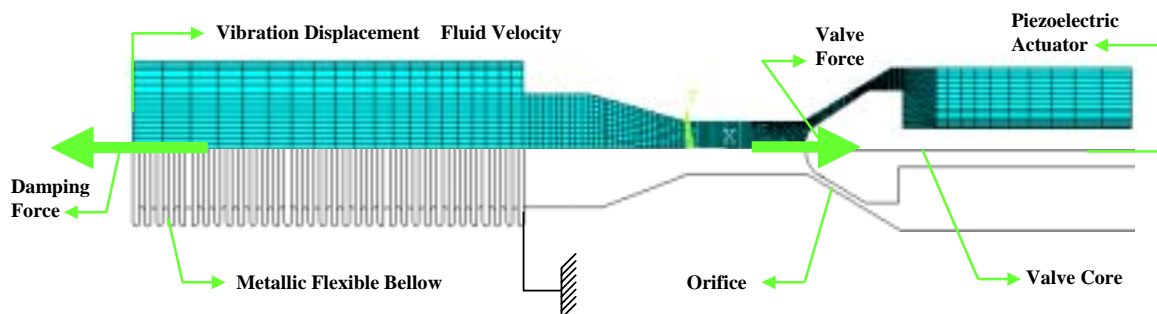


Figure 2. Finite element axi-symmetric model of the hydraulic circuit.

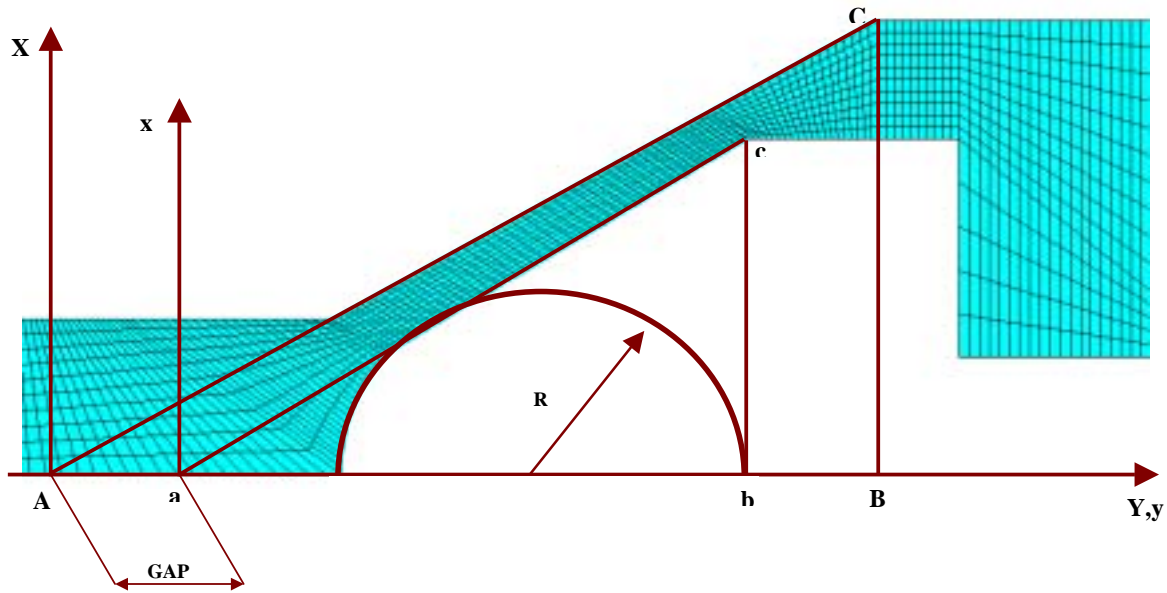


Figure 3. Valve geometry and mesh refinement

The working fluid is a Newtonian lubricant oil with density equal to  $8.42 \times 10^2 \text{ kg/m}^3$  and viscosity of a 0.0022 kg/ms. At all numeric simulations, the viscosity is considered to be temperature independent and the density is kept constant. The axial position of the conical core relative to the valve body is determined by the GAP variable measured at the X-axis of the inertial reference frame. As shown in Figure 3, GAP is the distance between the vertices of the triangles . abc and . ABC. The spherical tip of the core is generated by the circumference inscribed in the triangle . abc. The right end of the core has a cylindrical shape, where the actuator rod is fixed. If the reference frames XY and xy are coincident GAP results equal to zero and the valve is totally closed. The refinement of the mesh near the conical wall and the mesh geometrical transition applied this region of the model is also shown. Preliminary numerical simulations shown that the obtained Reynolds Number was low, so that the fluid flow can be considered laminar.

The applied boundary conditions are  $V_x = 0$  and  $V_y = 0$  at all internal walls, except at the left surface of the bellows. Due to the symmetry  $V_x = 0$  at the points where  $X = 0$ . Teixeira *et. al* (2003) show the field of velocities and pressures for simulations in the permanent regime and from the obtained results, the surfaces that maps the damping forces in function of the velocity and the GAP, were derived.

The Fig.4 shows the complete model, constituted by the two moving pistons and the rigid structure that contains the fluid. A displacement is imposed at the left piston and the right piston is attached to a spring with the same stiffness of the bellows.

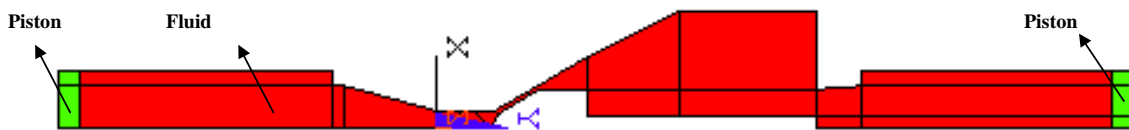


Figure 4: Areas of the Finite Element Model, which represent the fluid structure interaction.

The simulations are done for different GAP values, imposing a sinusoidal displacement with 3 mm amplitude at several frequencies, on the left piston, resulting the transient pressure and velocity fields. The net force at the valve core is calculated by integrating the pressure on the core surface. This force has to be supported by the piezoelectric actuator. The damping force applied to the vibrating structure is calculated by integrating the pressure over the area of the left bellows.

One of the variable required to the simulations is the oil bulk modulus, which represents the stiffness or the compressibility that the oil supports. To enter with the bulk modulus in ANSYS it is necessary to divide isentropic bulk modulus by the viscosity of the oil. Three different values were investigated for the Bulk modulus:  $8.42 \times 10^7$  (A),  $8.42 \times 10^6$  (B) and  $5.9782 \times 10^6$  (C) which require a specific time step to guarantee numeric convergence of the simulation. (0.0005, 0.01 and 0.01 seconds, respectively)

The problem modeled by fluid-structure interaction was solved by Eulerian-Lagrangean formulation (ALE), Donea *et. al.*(2004). This formulation it is made accordingly the flow chart illustrated on Figure 5. The algorithm starts the time solution with an initial mesh. The fluid-solid interaction solver solves the equations for the fluid and solid domains independently of each other. It transfers fluid forces and solid displacements across the fluid-solid interface. The mesh is updated and the algorithm continues to loop through the solid and fluid analyses until convergence is reached for that time step or until the maximum numbers of stagger iterations is reached. Convergence in the stagger loop is based on the physical quantities being transferred at the fluid-solid interface.

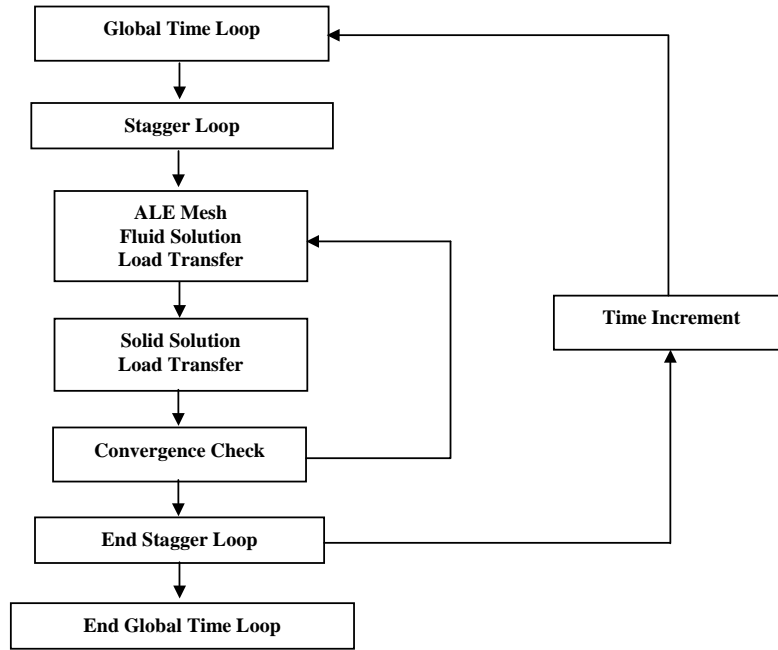


Figure 5: Lagrangean-Eulerian Algorithm.

### 3. Test with active damper device

Simulations results will be shown and compared with the results obtained experimentally. A total of 24 numeric simulations were made with GAP values of 0.06, 0.1, 0.15, 0.225, 0.35, 0.5, 0.75 and 1.00 mm, and with the three bulks modulus values.



Figure 6: Assembly of the active damper.

To properly operate the damper device must be filled with oil. Air bubbles must be removed and the fraction of solved gases in the oil must be low to avoid bulk modulus variation with the dynamic pressure. To achieve this task, the damper was filled out with oil using a vacuum pump, and two reservoirs, and a set of manual valves, as illustrated in the Fig.6. When the hydraulic damper was not admitting more oil, it was considered totally filled.

A static pressure sensor measured the internal system pressure of about 2 atm. The oil reservoirs were uncoupled after verifying that there was not any leak and the pressure indicated by sensor was steady. At this condition the damper is ready operate.

In the first experiments the damper is excited by an harmonic force at 5, 15 and 30 Hz using an electrodynamic shaker. In these tests, the damping force and the resulting velocity were measured at different GAP values. The force and velocity signals were captured by a computer based acquisition system. For those tests, the GAP position was set by a millimetric screw and measured by a dial gage.

The Fig.7 shows the experimental setup of the damper with the shaker coupled to the flexible bellows. A piezoelectric force sensor and an accelerometer measure the input signals applied to the damper. The input velocity at the bellows is obtained by analog integration of the acceleration signal.

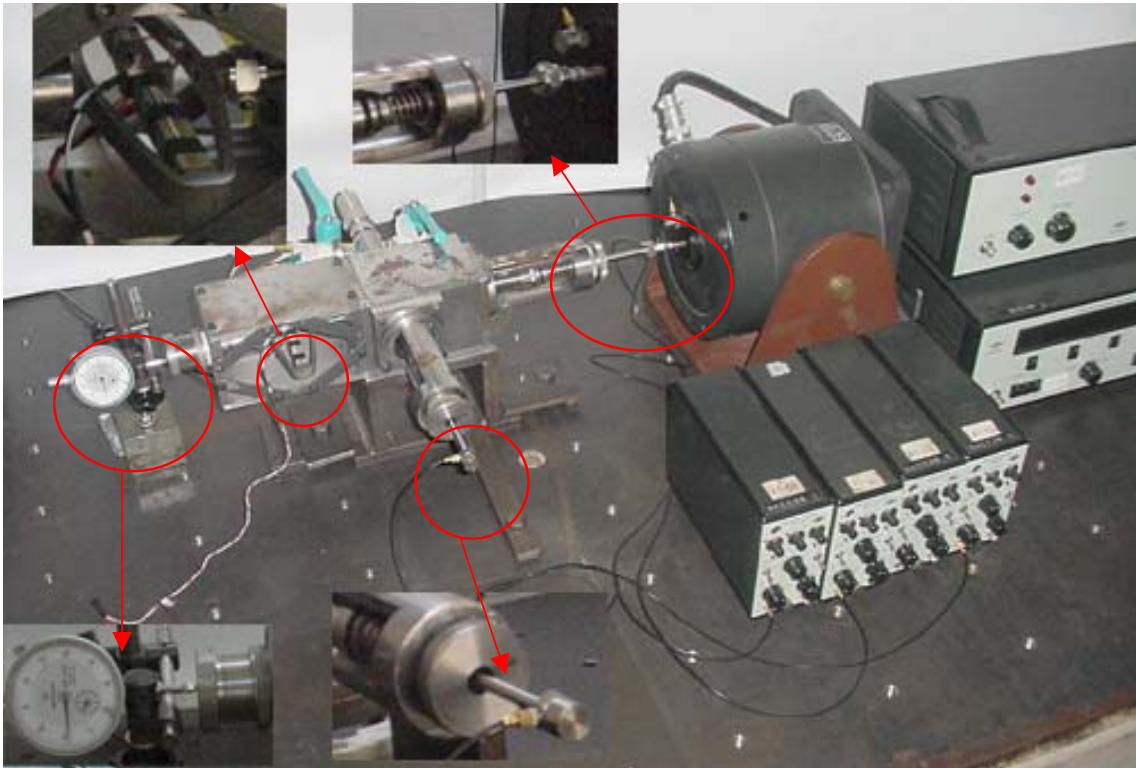


Figure 7: Experimental setup of the active damper with shaker coupled.

The results obtained for 20 investigated GAP values are shown in Fig.7, for the tests where the excitation frequency is 30 Hz. For each GAP value, velocity and damping force amplitudes were measured, resulting straight lines whose inclination is the damping coefficient.

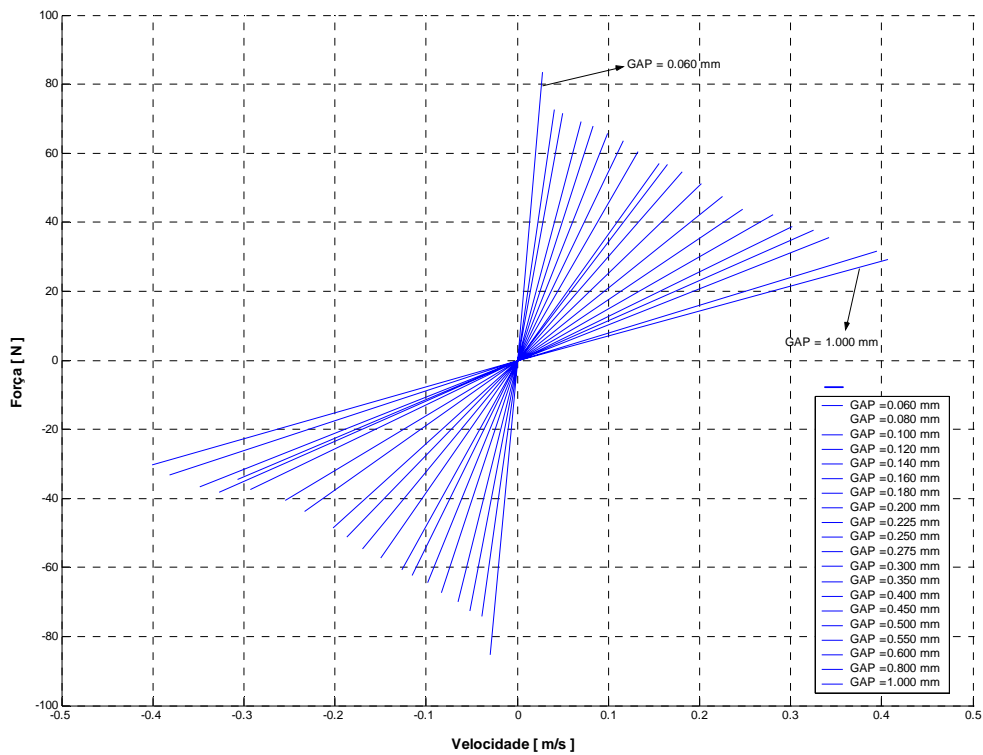


Figure 8: Experimental relation between the damping force and the velocity for different GAP values.

A frequency of 5 Hz was used at the computational simulations, using different values for the fluid bulk modulus. The inclination of the straight lines are related to the damping coefficients at each GAP, and are compared with the experimental results as shown by Fig.9.

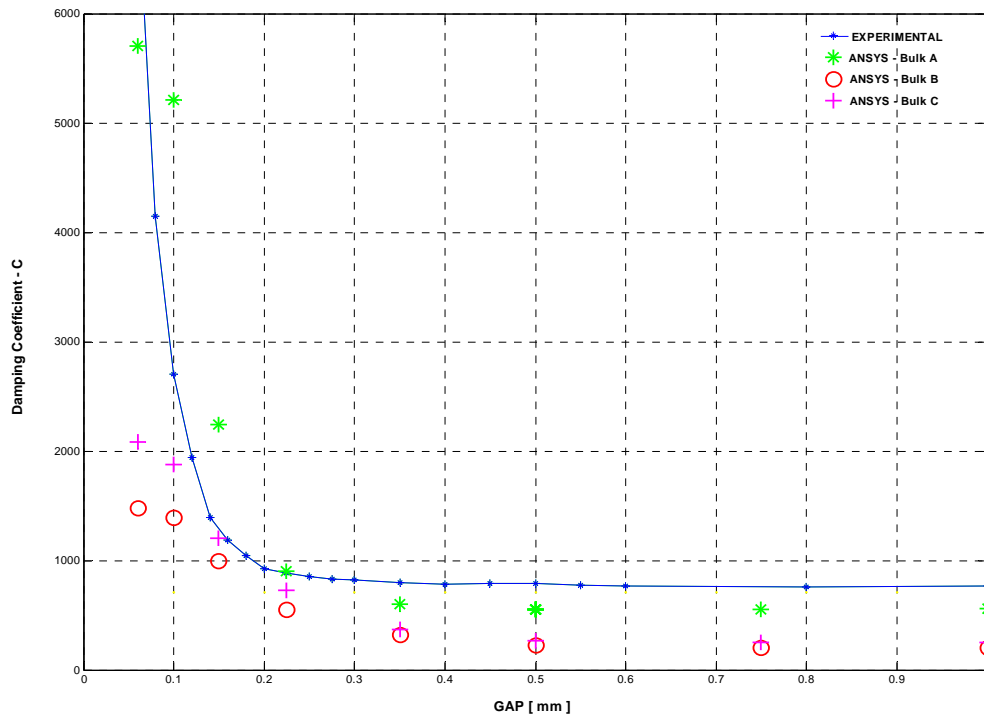


Figure 9: Comparison between the computational and experimental results for excitation in 5 Hz.

Fig.8 and Fig.9 indicate the damper linear behavior with the input velocity and also shows that the damping coefficient varies exponentially with GAP. Fig.9 shows that the damping coefficient is very sensitive on the value of the fluid bulk modulus in the computational simulations, and that there is a reasonable agreement between the numerical and experimental results for if a larger value is adopted. The computational finite element model becomes numerically unstable if the bulk modulus is further increased, even if integration time step is strongly reduced or a finer mesh is used in the fluid region. As a consequence of these numerical requirements, the computational effort is considerably increased and the direct use of this model is unpractical in real time control application.

In that way, the finite element model can be a reasonable tool to estimate the behavior of the damper and can be used to analyze the influence of changes on geometric and physical properties of the device on its dynamic characteristics.

#### 4. Active damper characterization on frequency domain.

Once the finite element model is validated with the experimental tests, it can be used to optimize the design of the damper, without the necessity to built new prototypes. The designer, with this model, will be able to study other configurations of valves, sizes of different bellows characteristics, and so on. However, for the design and operation of the piezoelectric actuator that dynamically sets the core valve position, the direct use of the finite element model becomes unviable due to the high computational time and cost.

A reduced model for the damper was used to represent the system on the frequency domain. The design of such system was achieved by experimental tests using a white noise excitation, in the band from 0 to 100 Hz applied to the left bellows and by measuring the force and the resulting accelerations on the left and right bellows. Some preliminary tests demonstrated that in the used frequency, the damper behaves like a second order system. The experiments were made for GAP values of 0.1, 0.15, 0.20, 0.25 and 0.30 mm. Fig.10 shows the bellows accelerations ratio and its phase difference. It is observed that for GAP values of equal and greater than 0.20 mm the gain between the two accelerometers is unitary and the phase difference is zero, indicating that the internal fluid acts like a rigid link between the two bellows and that the damper can be represented by a one degree of freedom system. The Fig.11 shows the punctual FRF at the excitation point, resulting the relation between the acceleration and the excitation force measured at the left bellows. In this same figure, the smooth curves are the adjusted FRF's used to estimate the model's physical properties, obtained by a multidimensional non-linear optimization process (Nelder-Mead method).

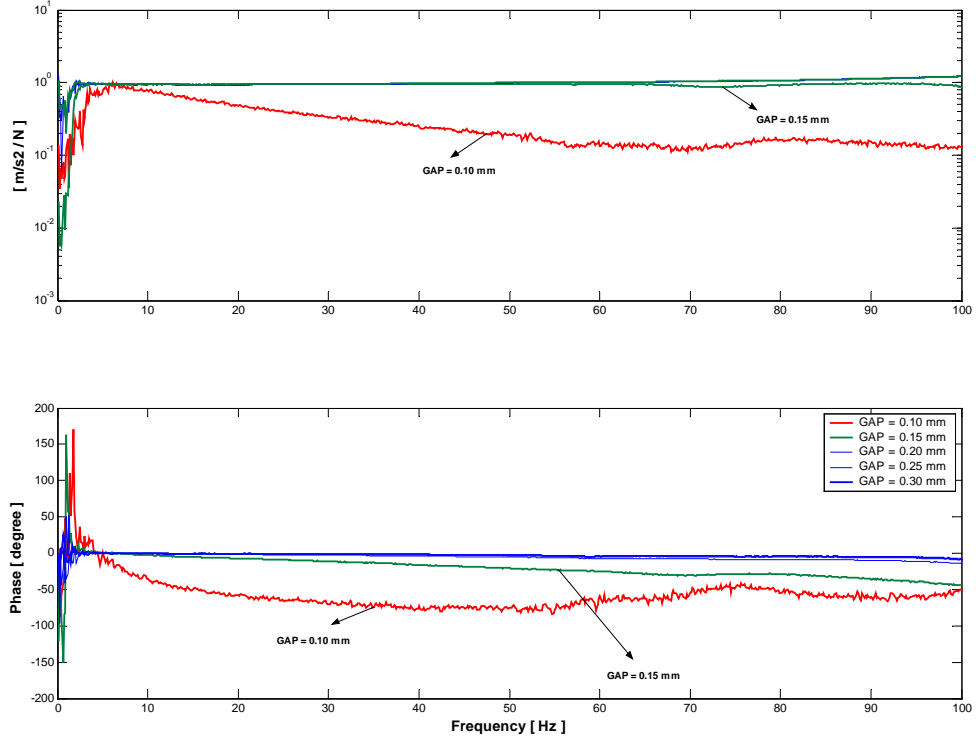


Figure 10: FRF's between the metallic bellows accelerations.

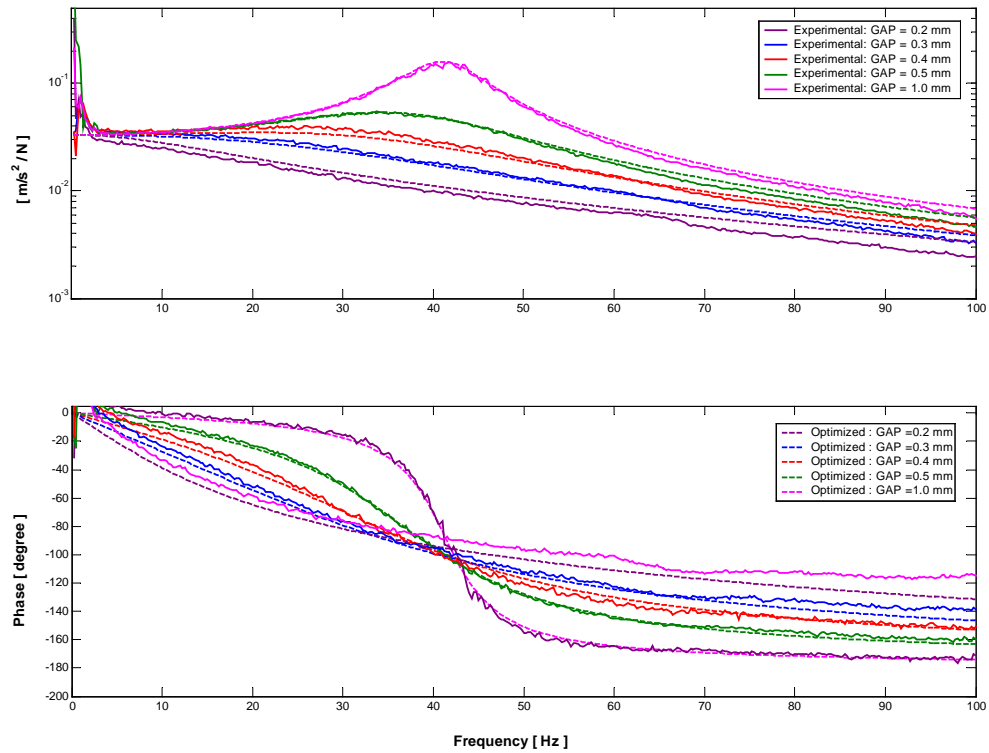


Figure 11: Experimental and Optimized FRF's for different GAP values.

## 5. Active damper with GAP fuzzy control.

In opposition to the classic logic, where the propositions assume only two values: false (0) or true (1), the fuzzy logic treats the propositions with different degrees of pertinence of values true or false. Teixeira (2001) made an overview of the fuzzy sets theory. The more important subject of the fuzzy controllers is the inference method, which is built and formulated through the fuzzy set theory. The inference method is based on a group of rules if-then that related some pertinence functions, which describe the variables of the system through linguistic variables.

The idea is to project a fuzzy controller such that given two inputs: the displacement (D) and the velocity (V) of the damper, the controller is capable to estimate the GAP to be imposed in the active damper in order to reach a certain performance index for the system state variables.

The first step of the fuzzy controller construction is to defined the physic input and output variables. The displacement and the velocity of the damper were adopted as input variables, and, the fuzzy controller output is the GAP that is, indirectly, the damping factor requested by the system. The universe of the discursion of variation of the variables were defined observing their ranges which are involved in the numeric simulations. Then, the input and output variable was partitioned by 5 gaussian pertinence functions, as illustrated in the Figure 12, which also describes the adopted base of rules. The base of rules is considered as the last stage of construction of the fuzzy controller and it was obtained by the designer intuition, after a series of numeric simulations.

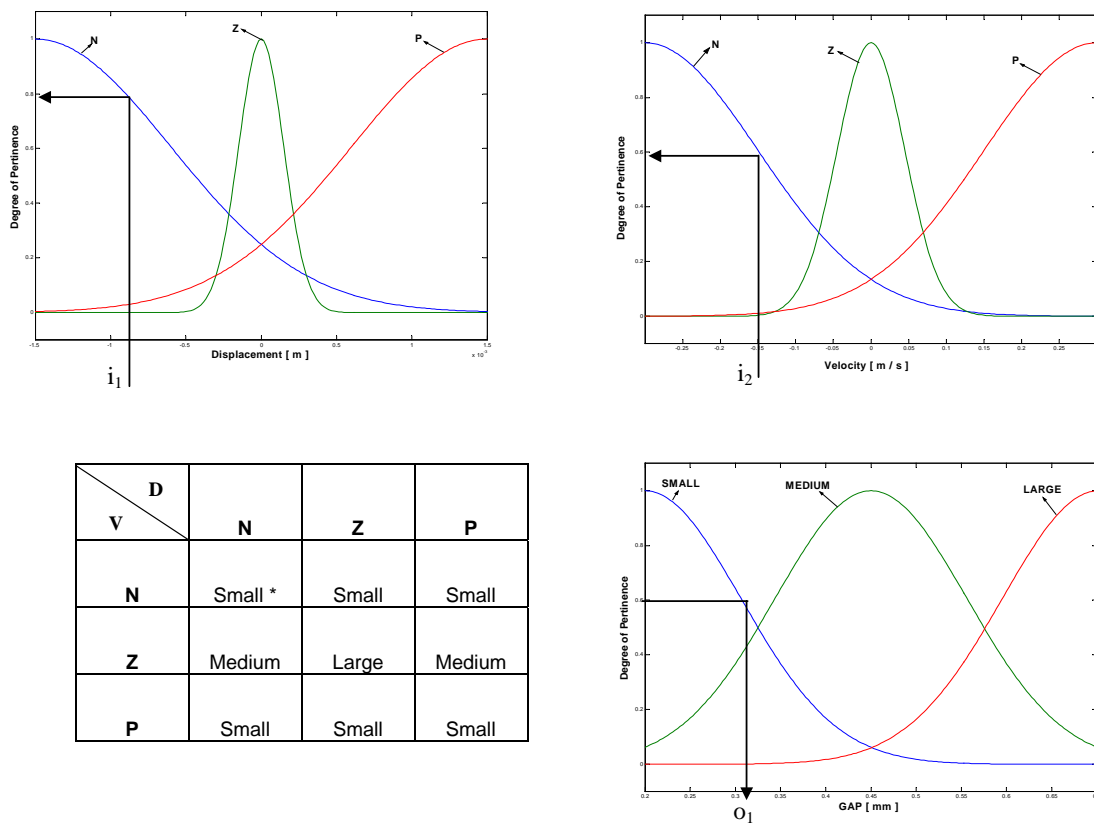


Figure 12: Inputs and output pertinence functions and rule base adopted.

For understanding the fuzzy algorithm type Mamdani considers the rule marked with (\*):

*If the displacement is Negative and the velocity is Negative, then GAP will be Small.*

Suppose, in a certain instant of time, the input displacement ( $i_1$ ) is -0.8 mm and the input velocity ( $i_2$ ) is -0.15 m/s. These values cut the pertinence functions in 0.8 and 0.6, respectively. Because the adopted inference method was the minimum between the degrees of pertinence of the two inputs, then 0.6 is the result of the fuzzification. The defuzzification enters with the value of 0.6 in the small GAP curve resulting the output ( $o_1$ ), that corresponds, in this instant of time, to GAP equal to 0.31 mm.

Using this fuzzy design, and the second order damper model identified in section 4, numerical simulations are done to evaluate the damper behavior. Both passive and active systems were submitted to an rectangular impulsive force with 300 N amplitude. The damper model is presented in the Equation 1, where  $K = 39.840$  N/m),  $\omega_n = 38$  Hz are,

respectively, the estimated stiffness and undamped natural frequency, and  $\zeta$  is the damping coefficient estimate, defined by Eq.(2).

$$G(s) = \frac{1}{K} \bullet \left( \frac{\zeta_n^2}{s^2 - 2\zeta_n s + \zeta_n^2} \right) \quad (1)$$

From the FRF's obtained and showed at Figure 11 it is possible to obtain, by an optimization process, the relation between the damping coefficient and GAP, which is described by Equation 2.

$$\zeta = 3.8252 \bullet e^{-6.2675 \cdot GAP} + 0.138 \bullet e^{-0.0046 \cdot GAP} \quad (2)$$

The passive system simulations used GAP = 0.45 mm, which is equivalent to a damping coefficient of 0.3656. In the active system, for to each instant of time (dt=1 ms), the fuzzy controller updates the GAP and consequently the damping coefficient value. Therefore, for the active system the transfer function of the system is modified for each instant. The displacements and velocities results for both cases are presented in the Figure 13.

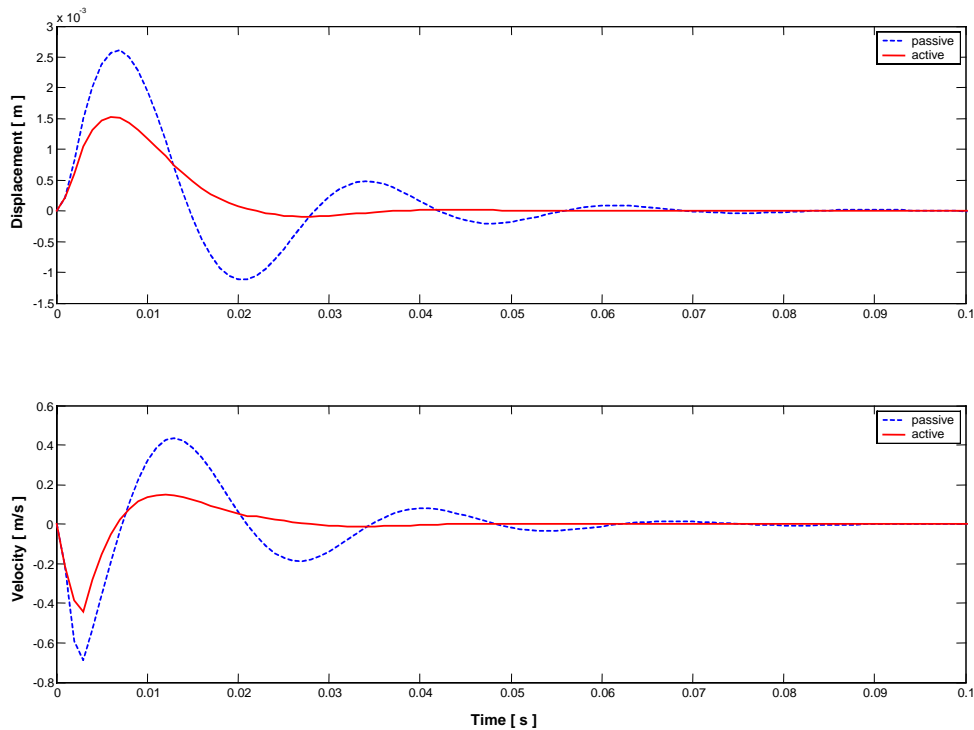


Figure 13: Displacement and velocity impulse response for the active and passive system.

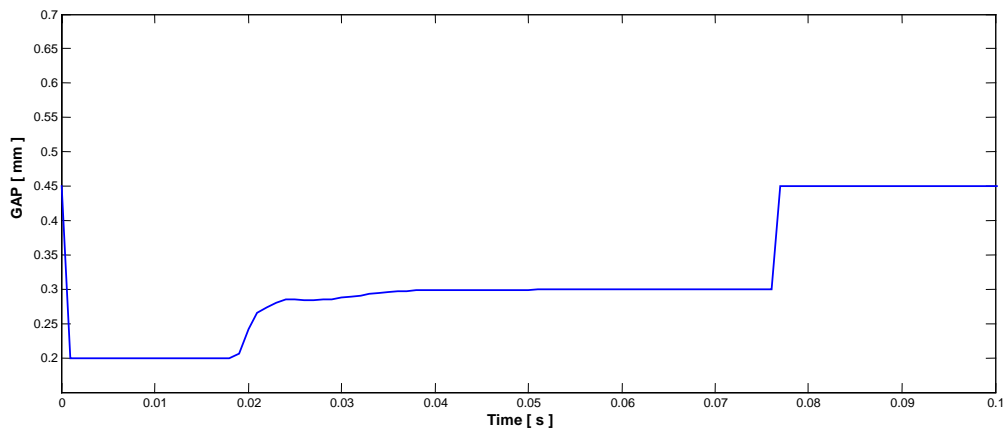


Figure 14: Gap updates for active system.

The Figure 14 show the behavior of GAP inferred by the fuzzy controller in the simulations with the active system, in other words, the piezoelectric actuator need to be supplied by a voltage that induces that behavior at the valve core. The piezoelectric actuator was not modeled, since it is not yet available, but its dynamics will be included in further work, and the complete control methodology will be verified experimentally.

## 6. Conclusions

The damper finite element model, which includes fluid-structure interaction, proved to be useful to analyze the device transient response and also shown the high numeric sensitivity with respect to the adopted value of the fluid bulk modulus. As shown by Fig. 9 a large value of this parameter resulted a better agreement with the experimental evaluation of the damping coefficient. The computational model becomes numerically unstable if the bulk modulus is further increased, even if integration time step is strongly reduced or a finer mesh is used in the fluid region. As a consequence of these numerical requirements, the computational effort is considerably increased and the direct use of this model is impractical in real time control application.

Otherwise, the adopted reduced damper model is suitable to represent the dynamical behavior of the device on a frequency band up to 100 Hz and for GAP values equal and greater than 0.2 mm. Using this model and the experimental frequency response functions, the damping factor estimate presents good approach of the computational and experimental models. The damping coefficient has exponential behavior with GAP and depends linearly on the velocity. Therefore, the damper dynamics is very sensitive to small changes of the GAP value. This is very important, for control applications since the piezoelectric actuator has a stroke range limited to 0.5 mm.

Future work will be done, including the experimental evaluation of the piezoelectric actuator and on the control strategy to be adopted in practical applications, as for example, vehicle and industrial equipment vibration control.

## 6. Acknowledgement

The authors thank the financial support from CAPES, CNPq and FAPEMIG, Brazilian agencies.

## 7. References

- Donea, J., Huerta, A., Ponthot, J.-Ph. and Ferran, A. R., 2004, "Chapter 14: Arbitrary Lagrangian–Eulerian Methods", Encyclopedia of Computational Mechanics, Edited by Erwin Stein, René de Borst and Thomas J.R. Hughes. Volume 1: Fundamentals. John Wiley & Sons, Ltd. ISBN: 0-470-84699-2.
- Giliomee, C.L. and Els, P.S., 1998, "Semi-active hydro pneumatic spring and damper system". Journal of Terramechanics 35, pp 109-117.
- Hagopian, J. Der, Gaudiller, L. and Maillard, 1999, "Hierarchical control of hydraulic active suspensions of a fast all-terrain military vehicle". Journal of Sound and Vibration 222(5),723-752. Article No. 1998.2082, available on line at <http://www.ideallibraty.com>
- Hyun-Ung Oh and Junjiro Onoda, 2002, "An experimental study of a semi active magneto-rheological fluid variable damper for vibration suppression of truss structures". Institute of physics publishing: Smart Materials and Structures 11, pp 156–162, available online at [stacks.iop.org/SMS/11/156](http://stacks.iop.org/SMS/11/156).
- Kitching, K.J., Cole, K.J., Cebon,D., 1998, " Performance of a semi-active damper for heavy vehicles", submitted to ASME Journal of Dynamic System Measurement and Control, June.
- Teixeira, R.L., Léopore, F. P., Ribeiro, J.F., 2003, "Active Damper System Design and Control – Part A and B", COBEM 2003: 170 Congresso Internacional de Engenharia Mecânica – São Paulo – Brasil.
- Teixeira, R.L., 2001, "Uma metodologia de projeto de controladores híbridos inteligentes com aplicações no controle ativo de vibrações mecânicas, Dissertação de Mestrado, Universidade Federal de Uberlândia – MG.

## 8. Copyright Notice

The authors are the only responsible for the printed material included in his paper.